Variable aggregation rates in colloidal gold: Kernel homogeneity dependence on aggregant concentration

B. J. Olivier and C. M. Sorensen
Department of Physics, Kansas State University, Manhattan, Kansas 66506
(Received 12 June 1989)

Dynamic light scattering is used to study the dependence of the aggregation kernel homogeneity λ on the aggregant concentration [HCl] for aqueous gold sols. We find the cluster growth kinetics are well described by a powerlaw, $R_{\rm app} \sim t^{z/D}$, where $R_{\rm app}$ is the measured apparent radius, D the cluster fractal dimension, and $z = 1/(1-\lambda)$ for all aggregant concentrations. The values for the dynamic exponent z, and hence the homogeneity λ, are functions of HCl concentration. We find the larger HCl concentrations yield a fast-aggregation regime characterized by $\lambda \simeq -0.6$. Smaller HCl concentrations yield a continuum of aggregation regimes characterized by homogeneities evolving from $\lambda \simeq -0.6$ towards 1.0. Our results do not support the view that aggregation in gold colloids is based on two limiting regimes, diffusion-limited and reaction-limited aggregation.

I. INTRODUCTION

Since the discovery of the fractal-cluster nature of the aggregate[1-3] and the dynamic scaling of the cluster size distribution,[4,5] the study of colloid aggregation has received intense and preserving interest. The focus of experimental study has illuminated the static and dynamic scaling properties of the fractal aggregates and their distributions in aqueous gold and silica sols.[6-11] These studies have indicated that two distinct aggregation regimes exist. They are the diffusion-limited (DLA) and the reaction-limited aggregation (RLA) regimes. DLA represents a fast colloid aggregation regime characterized by a power-law cluster growth,

$$R_H \sim t^{1/D} \tag{1}$$

where R_H is the mean hydrodynamic cluster radius and D the cluster fractal dimension. Conversely, RLA represents a slow regime characterized by exponential cluster growth,

$$R_H \sim e^{\alpha t} . \tag{2}$$

It is relevant to ask whether any intermediate regimes exist between these two, DLA and RLA, limiting regimes. Weitz, Huang, and Lin have suggested a crossover region may exist.[9] Here, initial cluster growth appears exponential (RLA), while final cluster growth appears power law as in Eq. (1) (DLA). Recently, Lin *et al.* have indicated that DLA and RLA comprise a two-regime universality for all colloids where the fastest and slowest aggregation regimes are DLA and RLA, respectively.[12,13] All their studies suggest that DLA and RLA are the only existing colloid aggregation regimes.

By contrast, in an earlier study of slowly aggregating aqueous gold sols we found power-law cluster growth as opposed to the expected exponential.[14] Furthermore, Wilcoxon, Martin, and Schaefer studied a fast-aggregation regime and found power-law behavior but with exponents uncharacteristic of DLA.[15] Neither of these studies supports earlier results from Weitz, Huang and Lin but instead suggest a more complex aggregation behavior. Stimulated by these discrepancies, we have decided to investigate systematically cluster growth rates as a function of aggregant concentrations in aqueous gold suspensions.

In this paper we report light-scattering measurements from aqueous gold sols to determine the aggregation kinetics as a function of aggregant concentration. By using dynamic light scattering as a probe, we have studied the temporal behavior of the first cumulant μ_1 of the homodyne intensity autocorrelation function.[16] The cluster growth rate is related to μ_1 by

$$\mu_1(t) \sim R_H(t)^{-1} \sim t^{-z/D} , \tag{3}$$

where the dynamic exponent z is related to kernel homogeneity through[5]

$$z = (1-\lambda)^{-1} . \tag{4}$$

By changing the molarity of our aggregant HCl, we were able to vary cluster growth rates, and hence the kinetic exponent z/D, over a wide range. Given the limited range of D found in the past, we were able to infer that the homogeneity λ varied with aggregant concentration. We found that the higher HCl concentrations yielded the quickest aggregation regime that was characterized with a kernel homogeneity significantly less than zero. This stands in contrast to the implication that the fastest aggregation regimes are DLA with $\lambda = 0$. Smaller HCl concentrations yielded a continuum of aggregation regimes characterized by kernel homogeneities evolving towards unity. This continuity of λ evolving with aggregant concentration is opposed to the two-regime description of aggregation with a crossover between. Rather, our results imply that a continuum of aggregation situations exist.

II. THEORY

The fundamental equation to describe aggregation kinetics in colloids is the Smoluchowski equation,[17]

$$\dot{n}=\tfrac{1}{2}\sum_{1+j=k}K(i,j)n_i n_j-n_k\sum_j K(k,j)n_j\ , \tag{5}$$

where $n_k(t)$ is the cluster size distribution describing the concentration of clusters with k monomers per cluster (concentration of k-mers) and $K(i,j)$ is the aggregation kernel describing the aggregation rate. Physical kernels usually appear as homogeneous functions of their arguments i and j, i.e.,

$$K(ai,aj)=a^{\lambda}K(i,j)\ , \tag{6}$$

where λ is the homogeneity.[5,18–20] In terms of kernel homogeneities, $\lambda=0$ and 1 define DLA and RLA, respectively. By assuming homogeneous kernels, similarity solutions to Eq. (5) lead to scaling cluster size distributions with the form[5]

$$n_k(t)\sim s^{-2}\phi(k/s)\ , \tag{7}$$

where the time dependence is found solely in the mean cluster size, $s(t)$.

The Smoluchowski equation is a mean-field approach to aggregation processes since concentration fluctuations are neglected. Qualitatively, after sufficiently long aggregation intervals, concentration fluctuations can dominate. This dominance is especially the case for aggregating fractal clusters having relatively large reactivities.[21] How good an approximation is the Smoluchowski equation is the relevant question to be asked here. In light of the lack of experimental evidence to answer this question, we proceed to use Smoluchowski's equation to predict the outcome of aggregation experiments since it is the best representation of aggregation we currently have.

We use the description of scaling given above in Eq. (7) along with dynamic light scattering (DLS) to characterize the aggregation kinetics in aqueous gold sols according to Eq. (5). With dynamic light scattering, we essentially measure the mean hydrodynamic radius R_H of the clusters as a function of time and use the scaling size distribution to characterize the $R_H(t)$ behavior.

Translation and rotation are two first-order diffusional processes which affect DLS spectra. Translational diffusion dominates, although rotational motion from the large, anisotropic fractal aggregates contributes significantly in the $qR_H\gtrsim 1$ regime, where q is the scattering wave vector. Therefore, proper interpretation of μ_1 to determine the dynamic behavior of R_H must include the effects from rotational motion.

A. Time evolution of scaled moments

Because μ_1 is an intensity weighted moment of the cluster size distribution, we integrate Smoluchowski's equation to determine the temporal behavior of moments in general. The time evolution of the Nth moment, M_N, is found by multiplying Eq. (5) by k^N and summing over k to yield

$$\dot{M}_N=\frac{1}{2}\sum_{i,j}[(i+j)^N-i^N-j^N]K(i,j)n_i n_j\ . \tag{8}$$

Following Taylor and Sorensen,[22] we assume the cluster size distribution has scaled, hence is represented by Eq. (7), and that the kernel is homogeneous with degree λ. Then,

$$\dot{M}_N=s(t)^{N+\lambda-2}I(K,\phi)\ , \tag{9}$$

where $I(K,\phi)$ is a constant dependent on $K(i,j)$ and $\phi(x)$. Notice that the time dependence of M_N rests solely in the temporal behavior of the mean size. This is not too surprising since the time dependence of the scaled distribution is governed by the same $s(t)$. By letting s represent the mass weighted mean cluster size in Eq. (9), i.e., $s=M_2/M_1$, an expression describing the evolution of s is found which upon substitution into Eq. (9) yields

$$M_N(t)=M_N(0)(1+t/t_c)^{(N-1)z}\ . \tag{10}$$

Here, t_c is a characteristic aggregation time related to the initial cluster size and kernel homogeneity, and z is given by Eq. (4).

We make the temporary assumption that the translational diffusion alone contributes to μ_1. In this case the first cumulant is given by

$$\mu_1=q^2\int D_k(k^2S_k)n_k dk\Big/\int(k^2S_k)n_k dk\ , \tag{11}$$

where k^2S_k is proportional to the amount of light scattered by a k-mer and D_k is the corresponding hydrodynamic diffusion coefficient

$$D_k=k_BT/6\pi\eta R_H\ . \tag{12}$$

Here, T represents the absolute temperature, η is the colloid viscosity, k_B is Boltzmann's constant, and R_H is the hydrodynamic radius of a k-mer. We use the well-found assumption $R_g\simeq R_H$,[23,24] thus $R_H\sim k^{1/D}$, so that $D_k\sim k^{-1/D}$ to obtain

$$\mu_1\sim q^2\int k^{2-1/D}S_k n_k dk\Big/\int k^2S_k n_k dk\ . \tag{13}$$

Finally, q is the scattered wave vector given by

$$q=(4\pi n/\lambda_0)\sin(\theta/2)\ , \tag{14}$$

where λ_0 equals the wavelength of light, n the colloid index of refraction, and θ the scattering angle.

To calculate the first cumulant we use the modified Fisher-Burford approximation for the scattering function,[25]

$$S_k=[1+(2/3D)q^2R_g^2]^{-D/2}\ . \tag{15}$$

and then consider the two limiting scattering regimes where S_k takes on its simplest forms. The first of these is the Rayleigh regime where $qR_H\ll 1$. Here, the scattering is isotropic and $S_k\simeq 1$. In this regime the amount of light scattered by a k-mer is proportional to k^2. With this, Eq. (13) yields

$$\mu_1\sim M_{2-1/D}/M_2 \tag{16}$$

and from Eq. (10) we obtain

$$\mu_1(t)=\mu_1(0)(1+t/t_c)^{-z/D} \tag{17}$$

for $qR_H\ll 1$.

The second regime is where $qR_H\gg 1$. In this regime the scattering has an angular dependence and

$S_k \simeq k^{-1} q^D$. At a fixed scattering angle, the amount of light scattered by a k-mer is proportional to k. Thus, in this regime Eq. (13) yields

$$\mu_1 \sim M_{1-1/D}/M_1 \tag{18}$$

and from Eq. (10) we obtain Eq. (17) for $qR_H \gg 1$ as well. Because $\mu_1 \sim R_H^{-1}$, we expect

$$R_H(t) = R_H(0)(1 + t/t_c)^{z/D} \tag{19}$$

in either limiting regime. With numerical calculations of Eq. (13) using the full expression for the structure factor, Eq. (15), we have found that Eq. (19) holds quite well in the intermediate regime $qR_H \sim 1$ as well; thus we will use Eq. (19) to analyze our data. For $t \gg t_c$ Eq. (19) yields $R_H(t) \sim t^{z/D}$ which is the expression usually used in the literature.[5-9] Finally, we remember that Eq. (19) is rigorous for translational diffusion alone.

B. Effects of rotational diffusion

When light scatters from fractal aggregates where $qR_H \gtrsim 1$, rotational diffusion significantly contributes to the decay rate of the autocorrelation function.[16,26] In this regime we no longer expect the inverse relation $\mu_1 \sim R_H^{-1}$ and one must account for the effects of rotational diffusion in the DLS spectrum. Therefore the validity of Eq. (19) must be further investigated.

The effects of rotational diffusion on a dynamic light-scattering experiment from fractal aggregates were recently studied by Lindsay *et al.*[26] In essence, they computer generated homodyne intensity autocorrelation functions from translational as well as rotational motions of clusters and calculated the corresponding first cumulants.

When performing an actual DLS experiment on an aggregating colloidal suspension, one may be uncertain of all relaxation modes contributing to μ_1. In the simple case of translational diffusion alone, μ_1 measures the mean hydrodynamic radius as

$$R_H = C_H q^2/\mu_1 , \tag{20}$$

where $C_H = k_B T/3\pi\eta$. When rotational diffusion may be present, and the clusters are anisotropic, Eq. (20) cannot be used to calculate a true hydrodynamic radius. In analogy to Eq. (20), however, an apparent radius may be defined as

$$R_{\text{app}} = C_H q^2/\mu_1 . \tag{21}$$

Using this definition, the results of Lindsay *et al.* are given in Fig. 1. They indicate the measured radius is the true hydrodynamic radius when $qR_H \ll 1$. As $qR_H \to 1$, rotational diffusion begins to affect the decay rate of the autocorrelation function and the measured radii appear smaller than the true hydrodynamic ones. At large qR_H, R_{app} is smaller than R_H by a constant factor. We can define a function $f(qR_H)$ by

$$R_H(t) = f(qR_H) R_{\text{app}}(t) , \tag{22a}$$

where

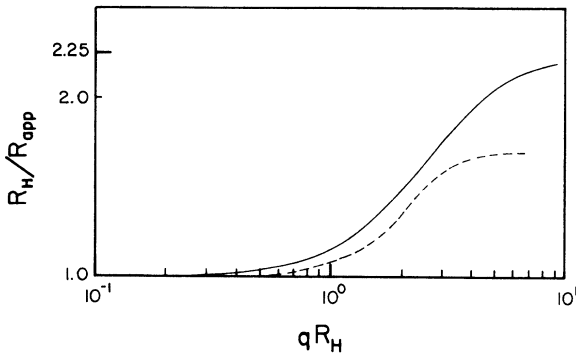

FIG. 1. The function $f(qR_H) = R_H/R_{\text{app}}$ vs qR_H. The dashed line is for a monodisperse system of fractal-cluster scatterers. The solid line includes the effects of polydispersity which results for a constant kernel aggregation process.

$$f(qR_H) = \begin{cases} 1, & qR_H \ll 1 \\ C, & qR_H \gg 1 . \end{cases} \tag{22b}$$

So long as $R_{\text{app}}(0)$ is large so that $qR_H > 1$ and $f(qR_H) = C$, then Eq. (19) may be written as

$$R_{\text{app}}(t) = R_{\text{app}}(0)(1 + t/t_c)^{z/D} . \tag{23}$$

III. EXPERIMENTAL METHOD

The gold colloid was prepared by sodium citrate reduction of chloroauric acid as described by Enustun and Turkevich.[27] A one-liter stock solution was made and all subsequent samples were taken from it. The stock solution was quasimonodisperse and had initial monomer of approximately 10 nm. Aggregation was initiated by the addition of HCl.

The experiments were carried out for two months raising the possibility that aging effects, where a change in the colloid stability, could appear. We measured equivalent aggregation rates using [HCl] = 0.132 M to aggregate sample sols at the start and finish of the two month span. Therefore, unlike the increased stability of an aging gold sol observed using pyridine as an aggregant, HCl yields no aging effect confirming earlier results from Wilcoxon, Martin, and Schaefer.

The dynamic light-scattering experiment was fairly standard.[16] Both argon ion, $\lambda_0 = 488$ nm, and helium neon, $\lambda_0 = 633$ nm, lasers were used to check for possible wavelength dependence of the observed aggregation dynamics. This is worthy of concern because the red to blue colored colloids absorb light. The measured kernel homogeneity λ showed no wavelength dependence which confirms the earlier work of Wilcoxon, Martin, and Schafer,[15] who also saw no wavelength effect on the dynamics of gold colloid aggregation.

The incident beam was split into two so that counter-propagating beams passed into the 1-cm^2 cuvette which was used as the scattering cell. By placing the detection photomultiplier tube (PMT) at an angle of 45° relative to these beams, we viewed the scattered light through a front wall of the cuvette. By blocking either one of the

two counterpropagating beams, scattering angles of 32° and 148° (accounting for refraction) were obtained. This arrangement gave us the ability to quickly change scattering angles, hence allowing us the luxury of investigating the angular dependence of the growth dynamics without halting the aggregation. The incident beam was vertically polarized and a polarizer at the front of the PMT accepted only vertically polarized scattered light.

The colloidal suspensions were carefully filtered through 0.22-μm millipore filters to remove dust. As a check of cleanliness, we required the measured monomer radii at 32° and 148° to be equal before aggregation. Possibly because of this filtration, the colloid concentration varied slightly from run to run. In the low [HCl] regime where the kinetics were very sensitive to both [HCl] and the gold concentration, some variation of the measured growth exponent z/D resulted for a given [HCl]. A few to several runs were made at each reported [HCl] to average this effect.

The scattering cell was equipped with a magnetic stirbar and mounted to top of a magnetic stirrer. To start a run the stirrer was turned on and HCl was injected into the colloid and stirred for 5 sec. The speed of the stirrer was fixed for all aggregated systems. This technique supplied a thorough, consistent mixing of the aggregant with the sol. Numerous runs were performed on the same colloidal stock suspension but with a variety of HCl concentrations ranging from 0.020 to 0.528 M.

The homodyne DLS spectra $C(t)$ were fit to the usual form[28]

$$C(t)=B+A\exp(-\mu_1 t+\tfrac{1}{2}\mu_2 t^2)\ , \tag{24}$$

where μ_1 and μ_2 are the first and second cumulants. μ_1 is the key quantity; the aggregation kinetics are contained in it as indicated above.

IV. RESULTS

We first describe DLS measurements on aggregating gold sols with relatively large HCl concentrations, [HCl]=0.132 and 0.033 M. Spectra were collected at scattering angles of 32° and 148° with λ_0=633-nm light. Using Eq. (21), apparent radii were calculated from the measured μ_1 and are plotted as a function of aggregation time for both angles in Fig. 2. DLS from a "simple" system, i.e., fairly monodispersed with only translational diffusion, should display q^2 dependence for μ_1 hence no dependence for $R_{\rm app}$ in which case $R_{\rm app}=R_H$. The data in Fig. 2 hint at a slight q dependence for $R_{\rm app}$ barely outside of experimental error near $t\lesssim 1000$ sec suggesting a more complex system.

In fact, as anticipated above, rotational effects are entering into the DLS spectra. Figure 3 shows the data from Fig. 2 along with one other run. To clearly illustrate the anomalous q dependence in the apparent cluster radius, we have plotted the ratio of radii measured at 32° and 148° against the measured radius at 32°. Representation of the data in this way eliminates the time variable thus allowing for intercomparison of runs. A ratio of unity would indicate that neither radius is q dependent. This is clearly not the case in Fig. 3, which shows a q

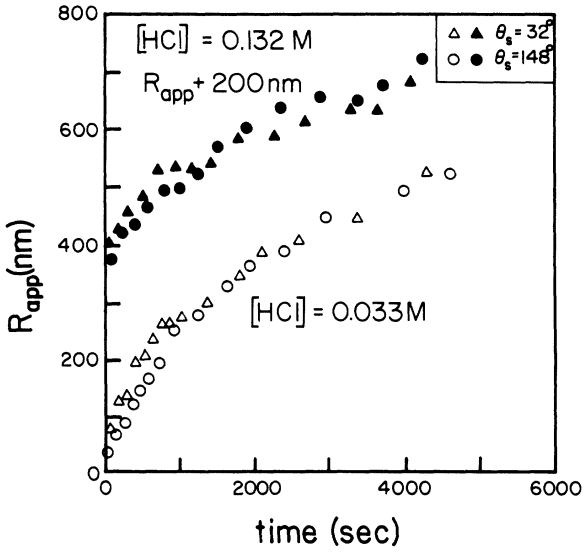

FIG. 2. Time evolution of the measured apparent radii at 32° and 148° for two runs with [HCl]=0.033 and 0.132 M.

dependence for $R_{\rm app}$ when $R_{\rm app}(32°)\lesssim 300$ nm.

This q-dependent radius or "hump" seen in Fig. 3 is due to the effect of both rotational and translational diffusion on the scattered light correlation function as described by Lindsay *et al.*[26] To see this qualitatively we refer back to Fig. 1 and Eq. (22) and write

$$\frac{R_{\rm app}(32°)}{R_{\rm app}(148°)}=\frac{f(q(148°)R_H)}{f(q(32°)R_H)}\ , \tag{25}$$

where $q(\theta)$ are the scattered wave vectors at the given scattering angles for λ_0=633 nm. For small qR_H, $f(32°)=f(148°)=1$, hence $R_{\rm app}(32°)/R_{\rm app}(148°)=1$. As

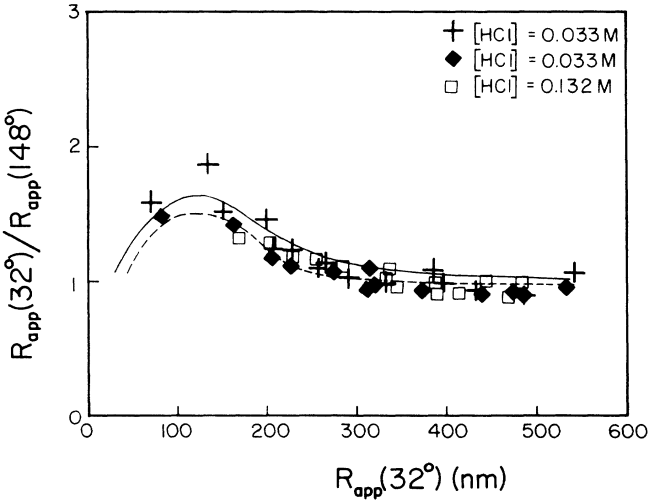

FIG. 3. Ratio of the measured apparent radii at 32° and 148° vs the measured radius at 32° for three different runs. The open squares and crosses represent the data from Fig. 2. The solid and dashed lines are the theoretical results including the effects of rotation from Fig. 1.

R_H grows, however, $f(148°)$ becomes greater than 1 before $f(32°)$; thus $R(32°)/R(148°)>1$, and the hump appears. This behavior continues until $qR_H>5$ where the f function begins to level off. When $q(32°)R_H>5$, $f(32°)=f(148°)=C$ and $R_{app}(32°)/R_{app}(148°)=1$ again. We have used the curves in Fig. 1 for $f(qR_H)$ to calculate $R_{app}(32°)/R_{app}(148°)$. The results are shown in Fig. 3 and are seen to fit the data well and hence support the theory of Lindsay *et al.*[26]

From these results we see that proper analysis of the data for the dynamic exponent z/D must either correct for rotational diffusion effects or find a qR_H regime where their effects are unimportant to the temporal growth behavior. Corrections will ultimately depend on the starting values of $q(\theta)R_H$. Ideally, one would stay in the region $qR_H<1$ where $R_{app}=R_H$. There rotational effects are ineffective and a useful study of aggregation kinetics could be obtained.[14] However, this is difficult to obtain because R_H grows to large sizes and small q (from small θ) is difficult to employ experimentally. On the other hand, when R_{app} is no longer q dependent, at large R past the hump in Fig. 3, $R_{app}(32°)=R_{app}(148°)=R_H/C$. Even if the value of C is unknown, $R_{app}(t)$ will yield the correct value of the exponent z/D as indicated in Eq. (23). In our analysis, we will both correct our data using the Lindsay *et al.* theory given by the solid curve in Fig. 1, and pay special attention to the data when R_{app} is no longer q dependent. We find that both procedures yield consistent results. Finally, we stress that this latter procedure yields the proper kinetics even when the theoretical correction breaks down.

A log-log representation of the [HCl]=0.132 M data in Fig. 2 is given in Fig. 4. We display the data with and without the rotational correction including polydispersity, the solid line in Fig. 1. The linearity suggests the data are well represented by

$$R_{app}(t)\sim t^{z/D} \tag{26}$$

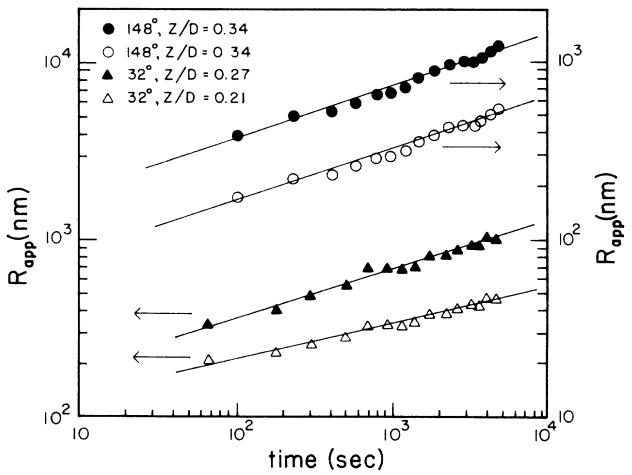

FIG. 4. Log-log representation of the growth of the measured apparent radii at 32° and 148°. The open figures are unadulerated data, the closed figures have been corrected for the effects of rotational motion. [HCl]=0.132 M.

indicating that $t\gg t_c$ in Eq. (23). The slopes represent the dynamic exponent z/D. The open figures are raw data, the solid figures are corrected for rotations as described above. The exponent z/D agrees for the corrected and uncorrected data at $\theta=148°$. We interpret this agreement to mean $f(q(148°)R_H)$ is already approximately constant at the start of our fit. To check this we use $C=2.25$ and calculate $R_H\simeq 405$ nm and $q(148°)R_H\simeq 10$ for our first data point. Figure 1 shows that for $q(\theta)R_H\simeq 10$, $f(q(\theta)R_H)$ is indeed a constant. At $\theta=32°$ the corrected and the uncorrected data yield values of z/D that differ by approximately 25%. Using $R_H\simeq 405$ nm, we calculate $q(32°)R_H\simeq 3$ indicating from Fig. 1 that $f(q(32°)R_H)$ is still changing. Hence rotational effects must be considered to properly infer the exponent z/D at $\theta=32°$. The corrected z/D at 32° (0.27 ± 0.04) is 20% below the z/D value obtained from the $\theta=148°$ data (0.34 ± 0.04). We found z/D at 32° below that at 148° for the other run for which both angles were used. Since this effect is on the edge of our experimental uncertainty, we are uncertain of its significance.

For five aggregation runs with [HCl]=0.132 M we found an averaged exponent of $z/D=0.33\pm0.04$ for both scattering angles. For aggregated gold clusters, the fractal dimension is bounded by $1.75\le D\le 2.05$. Since we have not measured D for the large variety of aggregant concentrations we have used, and since our uncertainty in the measured dynamic exponent, z/D, is larger than the spread in possible values for D, we choose $D=1.9\pm0.15$ to evaluate z and λ for all HCl concentrations. The range of z/D values which we shall report below makes the approximation of little consequence. Thus using $D=1.9$ we calculate an averaged kernel homogeneity of $\lambda=-0.6\pm0.2$. These results corroborate the earlier measurements made by Wilcoxon, Martin, and Schaefer,[15] who found $z/D=0.38$ and indicate a fast-aggregation regime in colloidal gold which is *not* DLA.

Similar results have been obtained for an entire aggregant concentration range of $0.05\ \text{M}\le[\text{HCl}]\le 0.528$ M. However, we have found that for [HCl] < 0.07 M the kernel homogeneity λ begins to evolve. A qualitative picture of the effects of HCl concentration on the dynamic exponent z/D is shown in Fig. 5, which gives a linear plot of the apparent radius against aggregation time. The distinct and different curvature of each data set suggests three different aggregation behaviors. Qualitatively, these curves may be described an increasing exponent z/D from left to right in the figure.

A log-log representation of the data in Fig. 5 is given in Fig. 6. To eliminate the need to correct for rotation, we consider only data in the $q(148°)R_H\gg 1$ regime. In this regime, $f(q(148°)R_H)\simeq C$. The linearity suggests the growth is power law and well represented by Eq. (26). The slopes in Fig. 6 are clearly different and lead to three distinct exponents given by $z/D=0.54$, 0.76, and 1.06 each with an uncertainty of ±0.05.

For similar colloidal gold suspensions Weitz, Huang, and Lin found that intermediate amounts of the aggregant pyridine led to a crossover behavior where initial cluster growth appeared exponential but ultimately

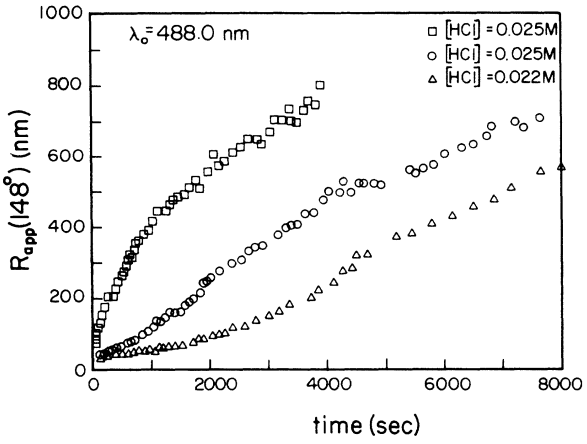

FIG. 5. Time evolution of the measured apparent radii at 148° for three different aggregation runs.

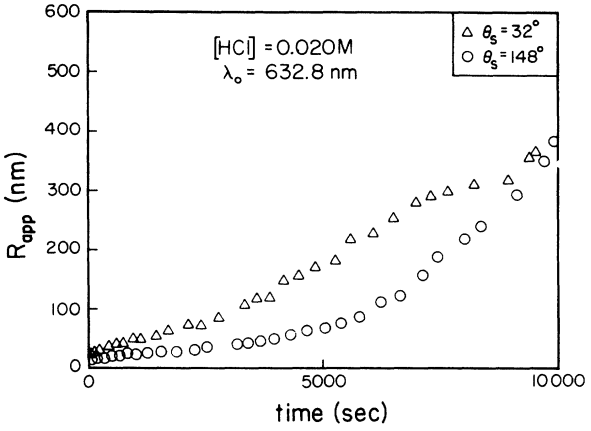

FIG. 7. Time evolution of the measured apparent radii at 32° and 148° for the run [HCl]=0.02 M.

crossed over to power-law growth at longer times characterized by the exponent $z/D \simeq 0.55$.[9] Semilog plots of our corrected data at early aggregation times are not linear, indicating our data do not show experimental growth at early times and a crossover is inconsistent with our data. Even if we disregard the early time data, we still do not reproduce the earlier work since we find power-law growth with exponents z/D distinctly different than 0.55.

Our lowest aggregant concentration, [HCl]=0.020 M, can at first be interpreted and displaying either exponential or power-law cluster growth. Figure 7 displays one of these runs showing R_{app} against aggregation time for the two scattering angles, 32° and 148°, and demonstrates a strong q dependence in R_{app}.

To compare these data to the q dependence predicted by the theory of Lindsay *et al.*,[26] we plot in Fig. 8 these data in the manner of Fig. 2. The large q dependence is substantiated by the large "hump" relative to the theory of Lindsay *et al.*

Evidently, something other than rotational and translational effects used in the Lindsay *et al.* theory is happening, but we cannot at this time say what. Whatever the source of this large hump, Fig. 8 is useful because it allows us to determine the range of data that yield a proper z/D via Eq. (23).

We note that the q dependence in $R_{app}(32°)$ disappears around 350 nm corresponding to $q(32°)R_{app}(32°) \geq 2.6$. We then assume that the q dependence in $R_{app}(148°)$ disappears at the same qR corresponding to $R_{app}(148°) \geq 100$ nm. Thus $R_{app}(148°)$ should yield an accurate determination of the kinetics when $R_{app} \geq 100$ nm.

Figure 9 is a semilog plot of $R_{app}(148°)$ versus time. No corrections can be made because, as Fig. 8 indicates, the Lindsay *et al.* theory does not work. Naively, one

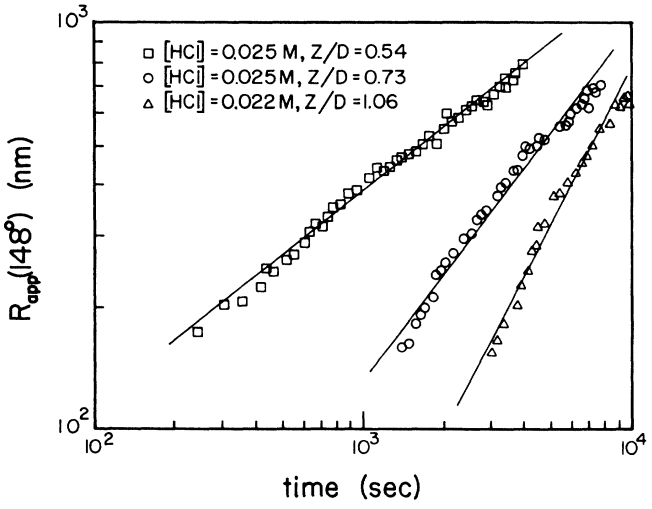

FIG. 6. Log-log representation of the growth of the apparent radii from Fig. 5. Only the data in the $qR_H \gg 1$ regime where $f(q(148°)R_H) \simeq C$ are considered.

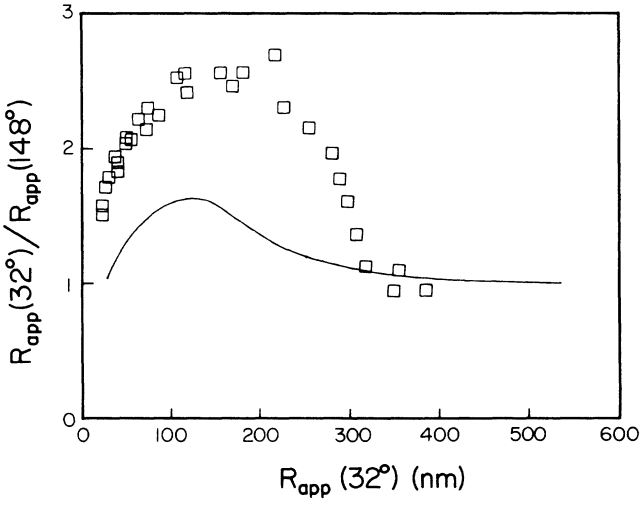

FIG. 8. Ratio of the measured radii at 32° and 148° vs the measured apparent radii at 32° for the data in Fig. 7. The solid line includes the effects of rotation from Fig. 1.

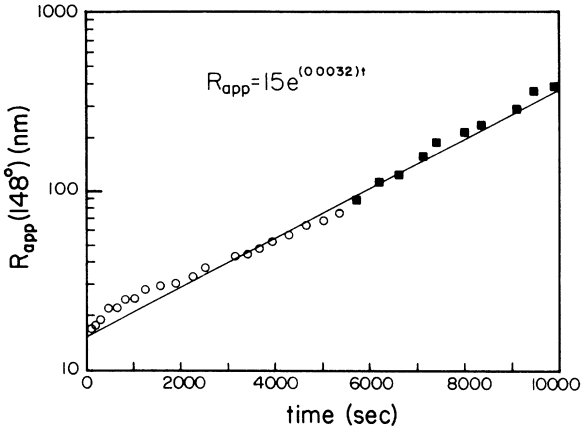

FIG. 9. Semilog representation of the apparent radius at 148° from Fig. 7. The solid figures are data where $f(q(148°)R_H)\simeq C$.

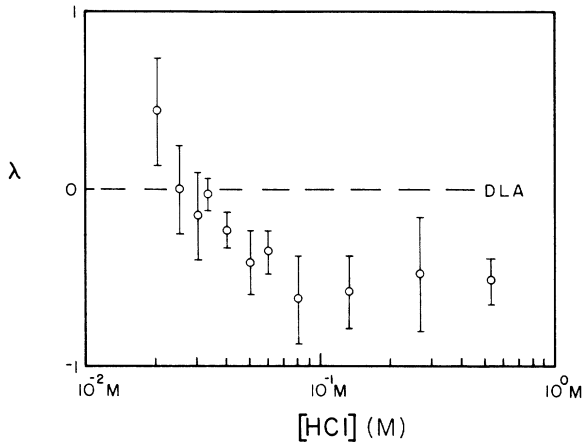

FIG. 11. The kernel homogeneity λ as a function of the aggregant concentration [HCl]. The dashed line represents diffusion-limited aggregation where $\lambda=0$. The error bars in this figure represent error in the measured z/D for a given run, the uncertainty in D, and run to run variation in z/D for a given [HCl].

would argue the linearity of all the data suggests exponential cluster growth where $R_{app}(t)\sim e^{\alpha t}$, but all the data cannot be used because they require an unknown correction. The solid points in Fig. 9 are for $R_{app}148\geq 100$ nm and require no correction to determine the kinetics as described above. They too are linear to imply exponential growth and we tentatively conclude this is a visible interpretation.

Figure 10 is a log-log representation of the data in Fig. 9. Again, no corrections can be made, but radii greater than 100 nm have no q dependence. Using just these q-independent radii, we find the dynamic exponent $z/D\simeq 2.7$ suggesting power-law cluster growth where $R_{app}(t)\sim t^{2.7}$.

We wish to argue in favor of a power-law cluster growth based on the return to q^2 dependence of the first cumulant late in the run. Using an analysis similar to Martin and Leyvraz,[29] we can show that any power-law cluster size distribution will yield a q dependence for the scattered light first cumulant with exponent greater than 2.[30] Since our first cumulant q dependence returns to q^2 after the hump in Fig. 8, our data suggest the cluster size distribution cannot be power law. Models of RLA and exponential growth,[10,31,32] however, have predicted power-law size distributions. The exactly solvable sum kernel, for instance, with $\lambda=1$ yields exponential growth with a power-law size distribution.[31] Thus exponential growth and non-q^2 dependence should occur together. Since we find q^2 dependence, the large power-law interpretation of the kinetics with $z/D=2.7$ is the most consistent interpretation.

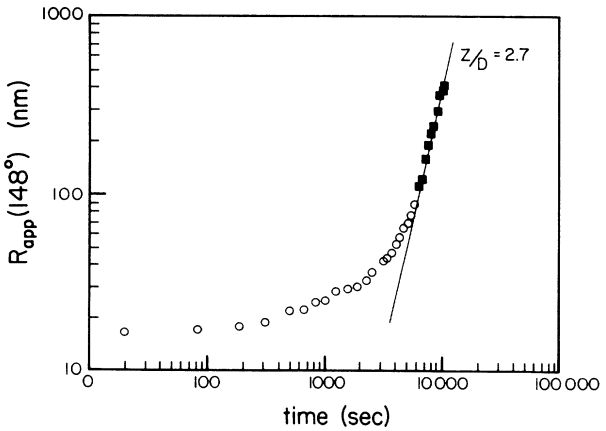

FIG. 10. Log-log representation of the apparent radius at 148° from Fig. 7. Again, the solid figures represent data where $f(q(148°)R_H)\simeq C$.

Our final result is given in Fig. 11, where we have plotted the kernel homogeneity λ as a function of HCl concentration. This figure represents the results of over 50 runs. Figure 11 convincingly demonstrates the evolution of λ. The fastest aggregation regime is characterized by $\lambda\simeq -0.6$. This regime does not represent DLA. We see, for smaller HCl concentrations, that λ does eventually evolve through $\lambda=0$ a value consistent with the diffusion-limited regime. At the lowest concentrations, λ does appear to be approaching unity, but RLA behavior, which we take to be both exponential growth and non-q^2 dependence, was not found.

V. CONCLUSIONS

We have used dynamic light scattering to study the growth kinetics during the aggregation of a gold colloid. We interpret our results in the context of the Smoluchowski equation to describe the observed aggregation kinetics. We have found that the aggregation kernel homogeneity is a continuous function of the aggregant concentrations. Our highest HCl concentration yielded $\lambda\simeq -0.6$, which is inconsistent with the anticipated $\lambda=0$ for diffusion-limited aggregation in the fastest aggregation regime. In fact, a limiting DLA regime does not exist in our colloid. The homogeneity increased as the aggregant concentration was lowered and appeared to approach 1, which should yield the exponential growth

characteristics of reaction-limited aggregation. Exponential growth was seen but the q dependence of the measured size was inconsistent with a power-law size distribution expected from RLA. Instead, our slowest aggregation regime was best described by a power law with a large exponent. Thus the aggregation kinetics in our colloids were not described by the simple view that only DLA and RLA regimes exist with a possible crossover between them, but rather displayed a continuum of aggregation kernel homogeneities.

ACKNOWLEDGMENTS

We wish to thank D. A. Weitz, M. Y. Lin, H. M. Lindsay, and J. P. Wilcoxon for useful discussions. Dr. Weitz and Dr. Lin kindly supplied numerical values for the rotational diffusion corrections. This work was supported by National Science Foundation Grant No. CBT8709622.

[1]T. A. Witten, Jr. and L. M. Sander, Phys. Rev. Lett. **47**, 1400 (1981).
[2]P. Meakin, Phys. Rev. Lett. **51**, 1119 (1983).
[3]M. Kolb, R. Botet, and R. Jullien, Phys. Rev. Lett. **51**, 1123 (1983).
[4]T. Vicsek and F. Family, Phys. Rev. Lett. **52**, 1669 (1984).
[5]P. G. J. van Dongen and M. H. Ernst, Phys. Rev. Lett. **54**, 1396 (1985).
[6]D. W. Schaefer, J. E. Martin, P. Wiltzius, and D. S. Cannell, Phys. Rev. Lett. **52**, 2371 (1984).
[7]D. A. Weitz, T. S. Huang, M. Y. Lin, and J. Sung, Phys. Rev. Lett. **53**, 1657 (1984).
[8]J. E. Martin and D. W. Schaefer, Phys. Rev. Lett. **53**, 2457 (1984).
[9]D. A. Weitz, T. S. Huang, M. Y. Lin, and J. Sung, Phys. Rev. Lett. **54**, 1416 (1985).
[10]D. A. Weitz and M. Y. Lin, Phys. Rev. Lett. **57**, 2037 (1986).
[11]J. E. Martin, Phys. Rev. A **36**, 3415 (1987).
[12]M. Y. Lin, H. M. Lindsay, D. A. Weitz, R. C. Ball, R. Klein, and P. Meakin (unpublished).
[13]M. Y. Lin, H. M. Lindsay, D. A. Weitz, R. C. Ball, R. Klein, and P. Meakin (unpublished).
[14]B. J. Olivier and C. M. Sorensen, J. Colloid Interface Sci. (to be published).
[15]J. P. Wilcoxon, J. E. Martin, and D. W. Schaefer, Phys. Rev. A **39**, 2675 (1989).
[16]B. J. Berne and R. Pecora, *Dynamic Light Scattering* (Wiley, New York, 1976).
[17]M. von Smoluchowski, Phys. Z **17**, 593 (1916).
[18]F. Leyvraz and H. R. Tschudi, J. Phys. A **15**, 1951 (1983).
[19]E. M. Hendricks, M. H. Ernst, and R. M. Ziff, J. Stat. Phys. **31**, 51 (1983).
[20]R. M. Ziff, M. H. Ernst, and E. M. Hendricks, J. Phys. A **16**, 2293 (1983).
[21]P. G. J. van Dongen, Phys. Rev. Lett. **63**, 1281 (1989).
[22]T. W. Taylor and C. M. Sorensen, Phys. Rev. A **36**, 5415 (1987).
[23]Z. Y. Chen, P. Meakin, and J. M. Deutch, Phys. Rev. Lett. **59**, 2121 (1987).
[24]P. Wiltzius, Phys. Rev. Lett. **58**, 710 (1987).
[25]M. E. Fisher and R. J. Burford, Phys. Rev. A **156**, 583 (1967).
[26]H. M. Lindsay, R. Klein, D. A. Weitz, M. Y. Lin, and P. Meakin, Phys. Rev. A **38**, 2614 (1988).
[27]B. V. Enustun and J. Turkevich, J. Am. Chem. Soc. **85**, 3317 (1963).
[28]D. E. Koppel, J. Chem. Phys. **57**, 4814 (1972).
[29]J. E. Martin and F. Leyvraz, Phys. Rev. A **34**, 2346 (1986).
[30]B. J. Olivier and C. M. Sorensen (unpublished).
[31]R. M. Ziff, in *Kinetics of Aggregation and Gelation,* edited by F. Family and D. P. Landau (North-Holland, Amsterdam, 1984).
[32]R. C. Ball, D. A. Weitz, T. A. Witten, and F. Leyvraz, Phys. Rev. Lett. **58**, 274 (1987).